

An investigation of dielectric properties of biological cells using RC-model

Sorawuth Bunthawin¹, Pikul Wanichapichart² and Jan Gimsa³

Abstract

Bunthawin, S., Wanichapichart, P. and Gimsa, J.

An investigation of dielectric properties of biological cells using RC-model

Songklanakarin J. Sci. Technol., 2007, 29(4) : 1163-1181

This paper proposes a method for estimating cell dielectric properties of a spherical triple shell and ellipsoidal shell models from the Laplace and RC approaches. With a combination of various theoretical parameters such as cell dielectrophoretic velocity, angular velocity of electro-rotation (ER) and two critical frequencies of dielectrophoresis (DEP), these approaches will improve the predictability of the dielectric properties. The calibration of the model parameters to these experimental data results in estimations of the cell's electrical properties depending on the geometric structure of the assumed model.

Key words : dielectrophoresis, ellipsoidal-shell model, RC-model, critical frequency

¹M.Sc. (Physics), Asst. Prof., Faculty of Technology and Environment, Prince of Songkla University, Phuket Campus, Kathu, Phuket, 83120 Thailand. ²Ph.D. (Biophysics), Assoc. Prof., Department of Physics, Faculty of Science, Prince of Songkla University, Hat Yai, Songkla, 90112 Thailand. ³Ph.D. (Biophysics), Prof., Chair of Biophysics, Department of Biology, University of Rostock, Gertrudenstr.11A, D-18057 Rostock, Germany.

Corresponding e-mail: pikul.v@psu.ac.th

Received, 29 April 2006 Accepted, 29 January 2007

บทคัดย่อ

สรุทธิ บุญถวิล¹ พิกุล วณิชชาติ² และ Jan Gimsa³
 การหาค่าสมบัติไดอิเล็กทริกของเซลล์ชีวภาพด้วยแบบจำลอง RC
 ว. สงขลานครินทร์ วทท. 2550 29(4) : 1163-1181

งานวิจัยนี้นำเสนอวิธีการประมาณค่าสมบัติไดอิเล็กทริกของเซลล์ตามแบบจำลองเซลล์ทรงกลมเปลือกสามชั้นและเซลล์ทรงรีด้วยวิธีลาปลาซ และวิธีแบบจำลอง RC กับพารามิเตอร์ทางกายภาพ อาทิ ความเร็วไดอิเล็กโตรฟอเรติก ความเร็วเชิงมุมในการหมุนตัวของเซลล์ และความถี่วิกฤตของ DEP ด้วยวิธีการเปรียบเทียบค่าที่คำนวณได้จากแบบจำลองกับค่าที่ได้จากผลการทดลองเหล่านี้ไปสู่การประมาณสมบัติทางไฟฟ้าของเซลล์ซึ่งขึ้นกับโครงสร้างโดยรวมของแบบจำลอง และหากนำผลของปรากฏการณ์เหล่านี้ไปใช้ร่วมกันจะทำให้การประเมินค่าสมบัติไดอิเล็กทริกมีความน่าเชื่อถือมากยิ่งขึ้น

¹คณะเทคโนโลยีและสิ่งแวดล้อม ภาควิชาวิศวกรรมเครื่องกล มหาวิทยาลัยสงขลานครินทร์ อำเภอเกาะพะงัน จังหวัดสุราษฎร์ธานี 83120 ²ภาควิชาฟิสิกส์ คณะวิทยาศาสตร์ มหาวิทยาลัยสงขลานครินทร์ อำเภอหาดใหญ่ จังหวัดสงขลา 90112 ³Chair of Biophysics, Department of Biology, University of Rostock, Gertrudenstr.11A, D-18057 Rostock, Germany

The phenomenon of dielectrophoresis (DEP) is the motion of particles or neutral matter due to polarization effects induced by non-uniform electric field (Pohl, 1978). It will only occur in the case that the electrical properties of the particle, i.e. its electrical conductivity and dielectric constant, differ from those of the suspending medium. As a result of this, the action of the applied electric field will be to induce electrical charges to appear at the boundary between the particle and the suspending medium. This was first described by Maxwell (1891) and further elaborated by Wagner (1914). The distortion of the electric field at the interface and the creation of Maxwell-Wagner interfacial charges lead to an electric dipole moment ($\vec{\mu}$) which depends on the electrical properties of the particles. Interactions between the induced dipole and electric field have been the subject of many investigations. The first publication that described the electrical impedance of cells in suspension was that by Cole (1928). This resulted in a number of studies of the motion of cells in electric fields (Holzafel *et al.*, 1982; Pohl, 1978, 1983; Chiabrera *et al.*, 1985; Fuhr and Kuzmin, 1986; Sauer, 1985; Kaler and Jones, 1990), of an electrical cell model (Pohl, 1978; Jones, 1995) and of a large number of applications in biotechnology, biomedicine

and pharmacology, such as the characterization of artificial or biological particles (Pethig and Markx, 1997; Mark and Davey, 1999), cell manipulation and separation (Pohl, 1978; Pohl and Hawk, 1978), electrically induced cell fusion (Zimmermann and Vienken, 1982). In our aspect, DEP is the phenomenon that has increasingly been applied to the study of the electrical properties of biological single cells (Irimajiri *et al.*, 1978; Hanai *et al.*, 1979; Asami *et al.*, 1984; Kaler and Jones, 1990; Raicu *et al.*, 1996, 1998).

In general, dielectric properties of micro scale single cells can directly not be measured. A cell suspended in a solution is assumed to be electrically neutral. When it is placed in a non-uniform AC electric field (\vec{E}), the induced dipole moment inside the cell interacts with the external electric force resulting in cell movements from an area of lower field intensity to an area of higher field intensity. This process is called positive "dielectrophoresis". A movement in the opposite direction is called negative DEP (Pohl, 1978; Jones, 1995). Moreover, mutual attraction among cells due to the dipole moment forms pearl chains and translation of the chains towards the electrodes might occur. If more than one cell species suspend in the same medium, positive and negative DEP

might occur simultaneously according to their electrical properties, leading to cell separation. To avoid cell-cell interaction, a single cell has carefully been selected and cell velocity recorded at a various field frequencies. Positive DEP at corresponding field frequencies were reported by Mahaworasilpa *et al.* (1994) and Wanichapichart *et al.* (2002). However, the method was rather tedious and time-consuming. The accuracy of the velocities obtained in such method was also questionable.

The force created as mentioned in the above process is called dielectrophoretic force (Scher, 1968; Pohl, 1978) which was defined as $\vec{F}_{DEP} = 0.5 \text{Re}[\vec{\mu}_{cell} \cdot \nabla \vec{E}^2]$, where $\text{Re}[\dots]$ represents real part of the complex function in the bracket and ∇ is the gradient operator. The dipole moment induced in the cell was defined as $\vec{\mu}_{cell} = \epsilon_0 \epsilon_s^* V [CMF] \vec{E}$, where ϵ_0 , ϵ_s^* and V represent permittivity of vacuum ($8.85 \times 10^{-12} \text{ F.m}^{-1}$), frequency dependent complex permittivity of the suspending medium and cell volume, respectively. CMF is the Clausius-Mossotti factor which is a frequency-dependent complex

function, i.e. $CMF = \frac{\epsilon_{eff}^* - \epsilon_s^*}{\epsilon_s^* + (\epsilon_{eff}^* - \epsilon_s^*) L_k}$, where ϵ_{eff}^*

and L_k is an effective complex permittivity of the whole cell and depolarization factor, respectively (Gimsa, 2004). Note that the CMF value is a determinant of the positive or the negative DEP, i.e. a positive CMF results in positive DEP and vice versa. These reveal that when the conductivity of the suspending medium (σ_s) is higher than the effective conductivity of a cell (σ_{eff}), the cell will experience a negative DEP force and be repelled from the electrode (negative DEP). When σ_s is lower than σ_{eff} the cell will be attracted to the electrode (positive DEP).

In some instance, the mutual attraction of cells with similar electrical properties will result in cell formation and pearl chains of cells. In the case of positive DEP, cells are accumulated at the electrodes, an effect that can be employed for cell selection and separation (Pohl *et al.*, 1978). Moreover, cells suspended in close proximity to one

another create phase-shifted field components resulting in the generation of a torque and, ($\vec{\tau}_{2-cell}$) hence, the rotation of the two cells in opposite directions (Mahaworasilpa *et al.*, 1996). Furthermore, when the electric field is produced by four different phases, a torque is easily induced on a single cell ($\vec{\tau}_{1-cell}$) (Gimsa *et al.*, 1991). Both of the effects, $\vec{\tau}_{1-cell}$ and $\vec{\tau}_{2-cell}$, can be described by the cross product $\vec{\tau}_{cell} = 0.5 \text{Re}[\vec{\mu}_{cell} \times \vec{E}^2]$. This phenomenon is well known as electro-rotation (ER). The two phenomena, DEP and ER, are part of the microelectromechanical systems of bio-particles (MEMS) (Jones, 2003).

The aforementioned description is based on the knowledge of the electrical cell properties such as conductivities and dielectric constants as well as the cell geometry. Many researchers employ a combination of different cell electro-mechanics methods (EMM) (Fuhr *et al.*, 1986; Fuhr and Kuzmin, 1986; Gimsa *et al.*, 1991; Mahaworasilpa *et al.*, 1996; Pohl and Crane, 1971) with dielectric spectroscopy (DSP) (Asami *et al.*, 1996; Asami, 2002; Gheorghiu, 1996) to improve the parameter resolution. Both methods have their advantages and drawbacks. The former can be applied to single cells. Nevertheless, it requires high intensity electric fields (kilovolt/meter) to induce cell translation or rotation. These fields may cause Joule-heating, a problem that can be reduced by lower conductivities of the suspension media or by the miniaturization of the measuring chamber (Gimsa *et al.*, 1996). However, the manipulation may still affect the electric properties of the cell (Schwan, 1988). The experimental data, such as the translation speed in DEP or the angular velocity in ER, are used in computing the electric cell properties. The latter is a non-invasive technique suitable for the characterization of suspended cells at low electric field intensities. Also, the method tends to be less time-consuming than the AC-EMM. However, electrode polarization at lower frequency is problematic. Studies of electric cell properties with DSP were limited until 1996 when Asami and co-workers developed scanning dielectric microscopy for the direct probing of cell clusters (Asami *et al.*,

1996). Their device consists of a dielectric probe, an impedance meter and a computer. It is commercially available, albeit at a high price. It might therefore not be suitable for preliminary studies.

DEP provides a cost-effective alternative. It is based on a number of measuring points for calculating the real part of the Clausius-Mossotti factor ($\text{Re}[\text{CMF}]$) from the models that fit the physical characteristics of cells being studied. Examples of these models are the spherical single shell model, SSM, for animal cells and plant protoplast (Kaler and Jones, 1990; Gimsa *et al.*, 1991) and the spherical double shell model, SDM, for certain animals' cells and plant cells possessing a cell wall (Asami and Irimajiri, 1984). These models are fundamental due to their geometries which are generally observed in cells. However, the models require a number of parameters concerning the dielectric properties of the cells (ϵ_{eff}^*). In addition, the DEP-function which varies with $\text{Re}[\text{CMF}]$ is not ad hoc available, resulting in difficulties in data fitting. The SSM model has therefore been introduced in a computer program by Bunthawin *et al.* (2003) to circumvent the manual calculations. However, the applicability of this model was limited to certain cell types such as plant protoplast and it was not valid for cells of a more general shape.

Not only the SSM and the SDM can be developed using the computing program, but also a spherical triple-shell model (STM). The same procedure as mention above has been applied, which is based on the Laplace solution (Bunthawin and Boonlamp, 2005). The electric potential and electric field have been calculated using the same theoretical analysis as given by Asami and Irimajiri (1984). Nevertheless converting this model into a multiple-shell model or ellipsoidal shell model using the same method might not be a simple undertaking due to mathematic complications. Moreover, for an ellipsoid, this approach raised the confocal shell problem, i.e. a layer of non-constant membrane thickness at poles of the cell is smaller than that at equatorial area. Therefore, another approach will also be made to

circumvent this problem.

Recently, Gimsa and Wachner (1998 and 1999) have warned about the use of confocal shells estimating that it may lead to large errors in the case of marked eccentricity. They proposed the RC-model for an ellipsoidal single shell model. The model consists of resistor-capacitor pairs which are commonly used to qualitatively describe relaxation processes and electrical properties of biological cells. The model is seems to be valid only under the assumption of constant field and consequently, only for shells of vanishing shell thickness. For thin (8-10 nm), low conductive shell, the model proposed by them has the great advantage of simplicity and can be useful for quantitative analysis of the CMF function and consequently, determining the critical frequency. This new approach emphasized two critical frequencies at transition points from negative to positive DEP and vice versa, represented as f_{cl} and f_{ch} , respectively. The two frequencies were plotted against medium conductivity (σ) and they gradually bended toward each other at high.

This work extends the RC approach to find a critical conductivity of the medium (σ_{ct}) which allows the two frequencies being in contact. It is envisaged that equations obtained for f_{cl} , f_{ch} and σ_{ct} will provide enough information to reveal cell dielectric properties and is a simpler method for experimentation

Modeling

a. The Laplace approach

The Laplace approach is a conventional method to determine electric field intensity both inside and outside the considered cell. This approach has been used for derivation of the effective complex permittivity of the whole cell including cell suspensions (ϵ_{eff}^*) which reveal cell dielectric properties in macroscopic view (Asami *et al.*, 1980; Asami and Irimajiri, 1984; Asami *et al.*, 1996; Asami, 2000). Previously, it was already known that the Laplace approach is nicely suitable for all spherical cell types (Pohl, 1978; Jones, 1995).

For our case the spherical triple shell model is also extended based on this approach. The cell model was set to be a solid sphere having radius (R), possessing inner cytoplasm (ic) located at the center covered by another inner membrane (im), outer compartment (oc), and outer membrane (om), respectively (Figure 1a). The thickness of each layer is defined by the radius distance (δ). Two-dimensional polar coordinates are employed for identifying any of interest position by the radius r and angles θ . Each component of the cell is described by its complex permittivity (ϵ_{eff}^*). The parameter of ϵ_{eff}^* can normally be calculated from the Laplace solutions and introduced into the CMF equation which is then separated into its $Re[CMF]$ and $Im[CMF]$ parts, respectively. This theoretical analysis gave the same result as Pohl (1978) and others (Bunthawin *et al.*, 2003; Bunthawin and Boonlamp, 2005). According to Pohl's assumption, the dipole moment induced in the cell strongly depended on the CMF. It is defined as $\vec{\mu}_{cell} = \epsilon_0 \epsilon_s^* V[CMF] \vec{E}$, where ϵ_0 and ϵ_s^* represent the permittivity of vacuum ($8.85 \times 10^{-12.5} F.m^{-1}$) and the frequency-dependent complex permittivity of the suspending medium, respectively. V stands for cell volume; note that, the volume of the spherical cell model with radius R and an ellipsoidal cell model with its semi-axe of a, b, c are equal to $\frac{4}{3} \pi R^3$ and $\frac{4}{3} \pi abc$, respectively. In case of ellipsoidal model proposed by Gimsa and Wachner (1999) the CMF can be written in generalized form as

$$CMF = \frac{\epsilon_{eff}^* - \epsilon_s^*}{\epsilon_s^* + (\epsilon_{eff}^* - \epsilon_s^*) L_k}, \quad (1)$$

where L_k is depolarization factor depending on cell shape. For a spherical case, $L_k = \frac{1}{3}$, then

$$CMF = \frac{3(\epsilon_{eff}^* - \epsilon_s^*)}{(\epsilon_{eff}^* + 2\epsilon_s^*)}. \quad (2)$$

One interesting case of an ellipsoid with two

equal semi-axes is known as the spheroidal model. For biological cell it has been developed by Watanabe *et al.* (1991) then by Kakutani *et al.* (1993) and Asami and Yonezawa (1995), respectively. They considered those spheroids of revolution with semi-axes of a, b and c ($a=b$) (Figure 1b), the inside of which is formed by another confocal spheroid with complex permittivity of cytoplasm of ϵ_c^* . This leaves an average clearance of δ between the two spheroid surfaces, the membrane characterized by ϵ_m^* . According to these models, ϵ_{eff}^* may be written in a complex form as Asami (2002)

$$\epsilon_{eff}^* = Re[\epsilon_{eff}^*] - j Im[\epsilon_{eff}^*], \quad (3)$$

where its real and imaginary part are

$$Re[\epsilon_{eff}^*] = \frac{\epsilon_o \omega \epsilon_m (AC + BD) - \sigma_m (BC - AD)}{\epsilon_o \omega (C^2 + D^2)}, \quad (4)$$

$$Im[\epsilon_{eff}^*] = \frac{\sigma_m (AC + BD) + \omega \epsilon_m \epsilon_o (BC - AD)}{\epsilon_o \omega (C^2 + D^2)}, \quad (5)$$

with these constants

$$A = \omega \epsilon_o (\beta_k (\epsilon_m - \nu (\epsilon_m - \epsilon_c)) + \epsilon_c),$$

$$B = \beta_k (\sigma_m - \nu (\sigma_m - \sigma_c)) + \sigma_c,$$

$$C = \omega \epsilon_o (\beta_k \epsilon_m + \epsilon_c + \nu (\epsilon_m - \epsilon_c)),$$

$$D = \beta_k \sigma_m + \nu (\sigma_m - \sigma_c) + \sigma_c,$$

where $\beta_k = \frac{1 - L_k}{L_k},$

$$\nu = \frac{1 - 3\delta}{\bar{R}},$$

and $\bar{R} = 3 \left(\frac{1}{a} + \frac{1}{b} + \frac{1}{c} \right)^{-1}.$

Substituting equation (3) to (5) and into equation (1) and (2) yields the final complicated expression of the CMF of the sphere and the ellipsoid which will be angular frequency (ω) dependent. Although the Laplace approach is a suitable analysis for

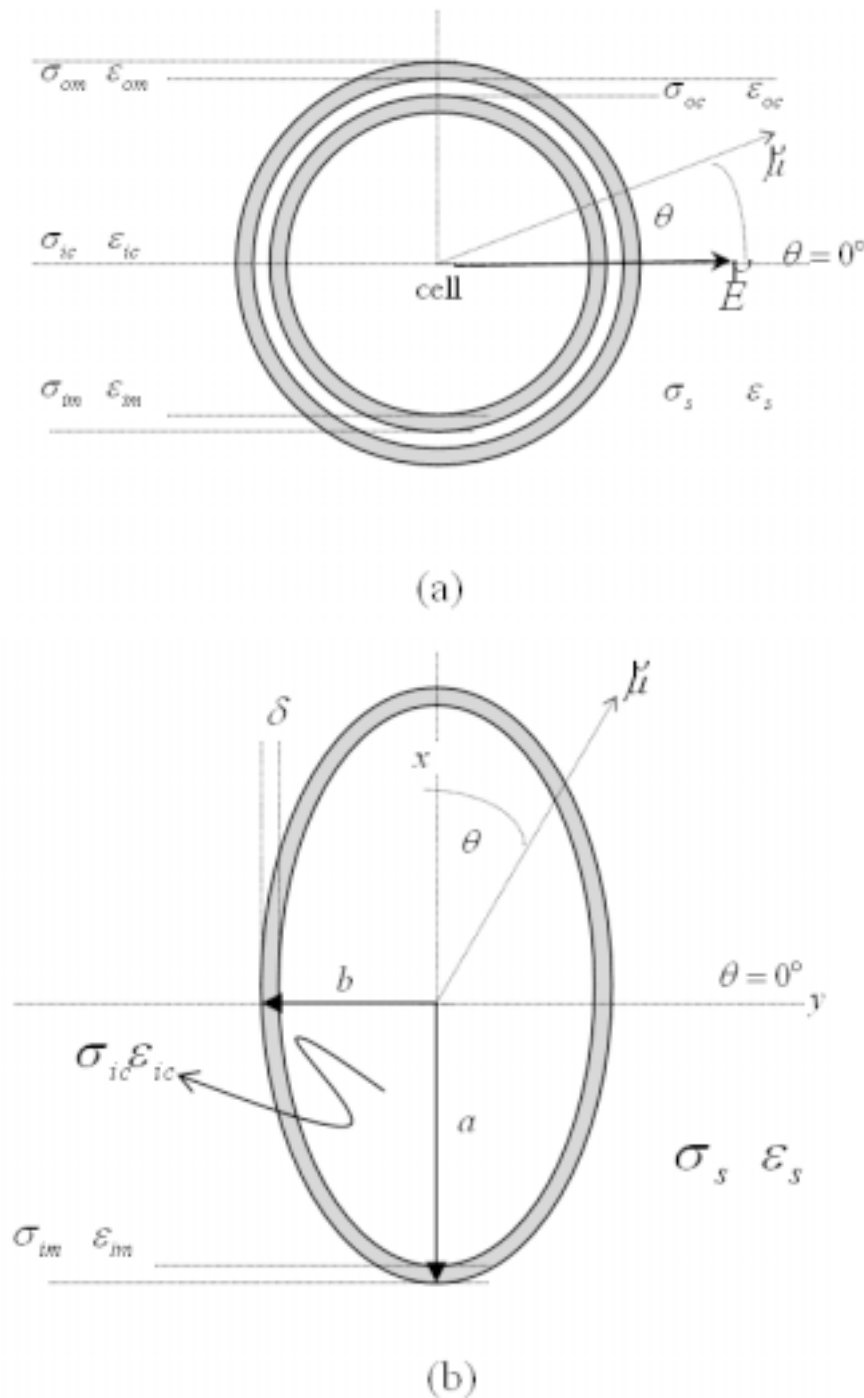


Figure 1. Two biological cell models represent a spherical triple shell model (STM) for a single cell (a) possessing three-dielectric layers with different dielectric properties and (b) an ellip-soidal single shell in case of two axis along y and z direction are equal. Both models are suspended in a low conducting medium with dielectric parameters of ϵ_s and σ_s . Dipole moment induced inside cells ($\vec{\mu}_{cell}$) will align itself parallel to the direction of external electric field (\vec{E}) at $\theta = 0^\circ$, resulting in positive dielectrophoresis.

computing all functions involving CMF based on the DEP method, applying the Laplace model to an ellipsoid raised the confocal shell problem, i.e. a layer of non-constant thickness modeling the biological membrane. This work also applied another approach developed by Gimsa and his colleague which employed an RC-model for calculating and (Gimsa and Wachner, 1998, 1999).

b. RC-approach

Previously, the ϵ_{eff}^* was originally deduced by using a Laplace approach, which was rather mathematically complicated. In case of ellipsoidal cell, the thicker membrane at the two poles than at the equatorial area brought about questions of validity. Therefore, another approach has been made by using an RC-model to correct the ambiguity about the membrane thickness (Gimsa and Wachner, 1998 and 1999). The CMF was modified

$$\text{as } CMF_{RC} = \frac{1}{L_k} \left(\frac{\psi_s^* - \psi_f^*}{\psi_s^*} \right), \text{ where } \psi_s^* \text{ and } \psi_f^* \text{ are}$$

electrical potentials of the medium and of the cell/medium interface, respectively.

In the following, each compartment of both models is assumed to be a conductive and capacitive property. The model of a spherical three-shells and ellipsoidal single-shell are shown in Figures 2a and 2b, respectively. When electric field is penetrating the cell membrane, it is equivalent to an electric current flow into a parallel circuit of a resistor-capacitor pair. This deduction represents the conductivity and permittivity of the membrane. In analogy, it can also be applied to cytoplasm and another compartment. The dielectric properties of phase (i) are determined by their complex function of conductive ($\sigma_i^* = \sigma_i + j\omega\epsilon_i\epsilon_o$) and capacitive ($C_i^* = \epsilon_i\epsilon_o A/\delta$), when σ_i and ϵ_i represent the DC conductivity and the relative permittivity of i phase. Then σ_i^* can be introduced into a complex function of specific impedance as $Z_i^* = (\sigma_i + j\omega\epsilon_o\epsilon_i)^{-1}$. For reasons already stated,

combining each phase in a series and introducing them into the CMF, yields a new function which will be impedance-dependent. According to Gimsa (2001), the polarization of an ellipsoid is assumed to be constant over cell volume, and the CMF factor along one semi-axis of the ellipsoid may be written

$$\text{as } CMF_{RC} = \frac{1}{L_k} \left[1 - \frac{Z_c^* + Z_m^*}{Z_c^* + Z_m^* + Z_s^*} (1 - L_k) \right]. \quad (6)$$

The subscript i denote phase of the cytoplasm (c) and the membrane (m). This approach can only not be applied to the ellipsoidal model but also to models of the spheroid and the spherical shape by changing the value of.

c. Critical and characteristic frequencies

In DEP critical frequencies, i.e. transition points from positive to negative DEP and vice versa, are observed. Characteristic frequencies, i.e. the rotation peak frequencies, occur in ER. We examined 5 prominent points in the DEP graph (Figure 3). The first point is the initial frequency when the DEP started at lower frequency range. The second is the final frequency where DEP ceases at high frequencies. The third is the frequency where the cell exhibits positive DEP with the highest amplitude. The fourth and the fifth are the frequencies at which the cell exhibits negative DEP in the lower and the higher frequency range, respectively. To consider these points through equation (6) and (2) is quite complex and our lack of advanced mathematic skills required for modeling spheroid cells poses a problem. However, we had already assigned the CMF term to equation (6). This could be a new method and an alternative to the conventional Laplace approach. From the model the dielectric properties of the membrane are prominent in the low frequencies range, namely, $Z_m^* = (\sigma_m + j\omega\epsilon_o\epsilon_m)^{-1}$, $Z_c^* = (\sigma_c)^{-1}$, and $Z_s^* = (\sigma_s)^{-1}$. On the other hand, those of the cytoplasm are dominant in the higher frequency range, $Z_m^* = 0$, $Z_c^* = (\sigma_c + j\omega\epsilon_o\epsilon_c)^{-1}$, and $Z_s^* = (\sigma_s + j\omega\epsilon_o\epsilon_s)^{-1}$. For these assumptions we can simplify the RC

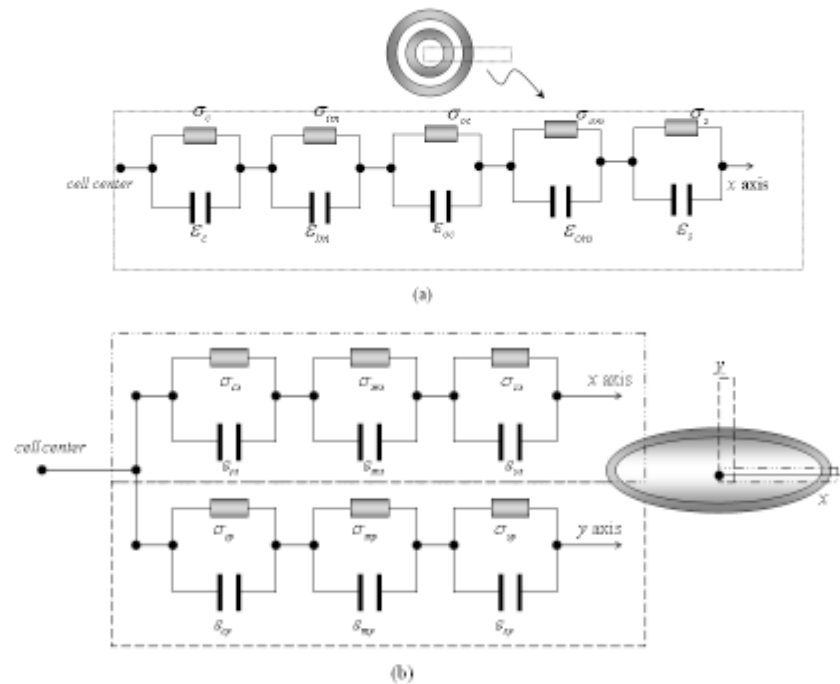


Figure 2. Equivalent RC models of (a) the spherical three-shell model and (b) ellipsoidal single-shell model shown in Fig. 1a and 1b, respectively.

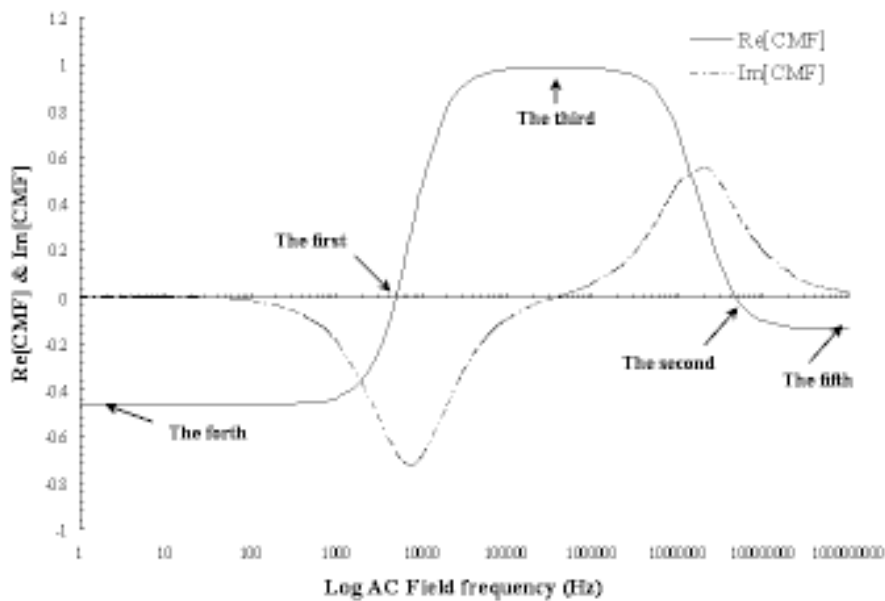


Figure 3. The prominent points shown on the theoretical plots of Re[CMF] and Im [CMF] of spherical triple shell model versus logarithm of field frequency for the following parameters : $R = 20 \mu m$, $\epsilon_{ic} = \epsilon_{oc} = 78$, $\epsilon_{im} = \epsilon_{om} = 8$, $\epsilon_s = 80$, $\sigma_s = 0.1$, $\sigma_{ic} = \sigma_{oc} = 0.4$, $\sigma_{im} = 0.1 \mu S.m^{-1}$, $\sigma_{om} = 1 \mu S.m^{-1}$

circuit schemes for the derivation of critical frequencies as shown in Figure 4a (f_{cl} at low frequencies) and Figure 4b (f_{ch} at high frequencies). Theoretical statements of these simplifications are

$$CMF_{RC}^l = \frac{(\sigma_s + \sigma_c + Z_m^* \sigma_s \sigma_c - \sigma_s \alpha - \sigma_s \sigma_c \alpha Z_m^*)}{(\sigma_s + \sigma_c + Z_m^* \sigma_s \sigma_c) L_k} \quad (7)$$

and

$$CMF_{RC}^h = \frac{(1 - \alpha) Z_c^* + Z_s^*}{(Z_c^* + Z_s^*) L_k} \quad (8)$$

where $\alpha = \left(\frac{1}{1 - L_k} \right)$. Note that these CMF equations are impedance-dependent functions which vary with angular frequency ($\omega = 2\pi f$). To determine f_l and f_h , the real parts of equation (7) and (8) are set to zero i.e. $\text{Re}[CMF_{RC}] = 0$, then w will be transposed from the equation. It was found that those equations can be written in the form of polynomials function as $a_n w^n + a_{n-1} w^{n-1} + \dots + a_0 = 0$, which will easily be solved using extraction of n root. The results are shown as follows:

$$f_{ch} = \frac{\varepsilon_o \sqrt{-AB}}{2\pi C} \quad \text{and} \quad f_{cl} = \frac{\varepsilon_o \sqrt{-E(F+G)}}{2\pi D}, \quad (9)$$

where

$$\begin{aligned} A &= -\varepsilon_c^2 - 2\varepsilon_c \varepsilon_s + \varepsilon_c \varepsilon_s \beta + \varepsilon_s^2 \beta - \varepsilon_s^2, \\ B &= -\sigma_c^2 - \beta \sigma_s^2 + \sigma_c \sigma_s \beta - \sigma_s^2 - 2\sigma_c \sigma_s, \\ C &= \varepsilon_o^2 A, \quad D = \varepsilon_m \varepsilon_o^2 E, \\ E &= \beta \sigma_s \sigma_c - \sigma_c^2 + \beta \sigma_s^2 - 2\sigma_c \sigma_s - \sigma_s^2, \\ F &= 2\beta \sigma_m \sigma_c \sigma_s^2 + \sigma_c^2 \sigma_s \sigma_m \beta - \\ &\quad 2\sigma_c \sigma_s \sigma_m^2 - \sigma_c^2 \sigma_s^2 - 2\sigma_c \sigma_m \sigma_s^2 - \sigma_m^2 \sigma_s^2) \\ G &= \beta (\sigma_m^2 \sigma_s^2 + \sigma_c^2 \sigma_s^2 + \sigma_c \sigma_s \sigma_m^2) - \\ &\quad \sigma_c^2 \sigma_m^2 - 2\sigma_s \sigma_m \sigma_c^2 \end{aligned}$$

If $f_{cl} = f_{ch}$, the σ_s can be solved and is called the critical frequency (σ_{ct}).

$$\sigma_{ct} = \frac{\sigma_c(2-\beta)}{2(\beta-1)} \quad \text{and} \quad \beta = \frac{1}{(1-L_k)}, \quad (10)$$

where

$$L_x = -\frac{1}{q^2 - 1} + \frac{q}{(q^2 - 1)^{3/2}} \ln[q + (q^2 - 1)^{1/2}]$$

$$\text{and } q = \frac{a}{b}.$$

Experimental

a. Cell preparation

Yeast cells, *Saccharomyces cervisiae* TISTR 5088, were used in this study. They were grown in an aqueous medium containing 39 g. ℓ^{-1} of Potato Dextrose Agar (PDA, Criterion) at 27°C in an incubator-shaker (Jecons Scientific) at 200 rpm. They were harvested in the stationary phase at 24 h after inoculation and washed one time in deionized water following centrifugation at 100 g for 2 min. Then the washed yeasts were twice washed in 0.8 M sorbitol. They were then re-suspended in the sorbitol with its conductivity adjusted from 3 mS.m⁻¹ to 0.3 S.m⁻¹ using 0.1 M KC ℓ . Experimentation was carried out at room temperature, 25.8° ± 1.2 C. Only one cell was placed in between nickel alloy cylindrical electrodes. Under a frequency range between 100 Hz to 1 MHz, the f_{ch} was not detectable and the f_{cl} was recorded at field strength of 85 kV.m⁻¹. The f_{cl} shifted to a higher frequency value with a decrease in positive DEP, and the σ_s was increased. In the σ_s range used, about 10 duplicates were carried out and the f_{cl} and f_{ch} were recorded within 20 min.

b. Electric field requirements

Another important aspect is the alignment of the electrodes used in DEP and ER studies. It determines the intensity and direction of the electric field. The orientation of the electric field determines the direction of cell translation or rotation. In DEP

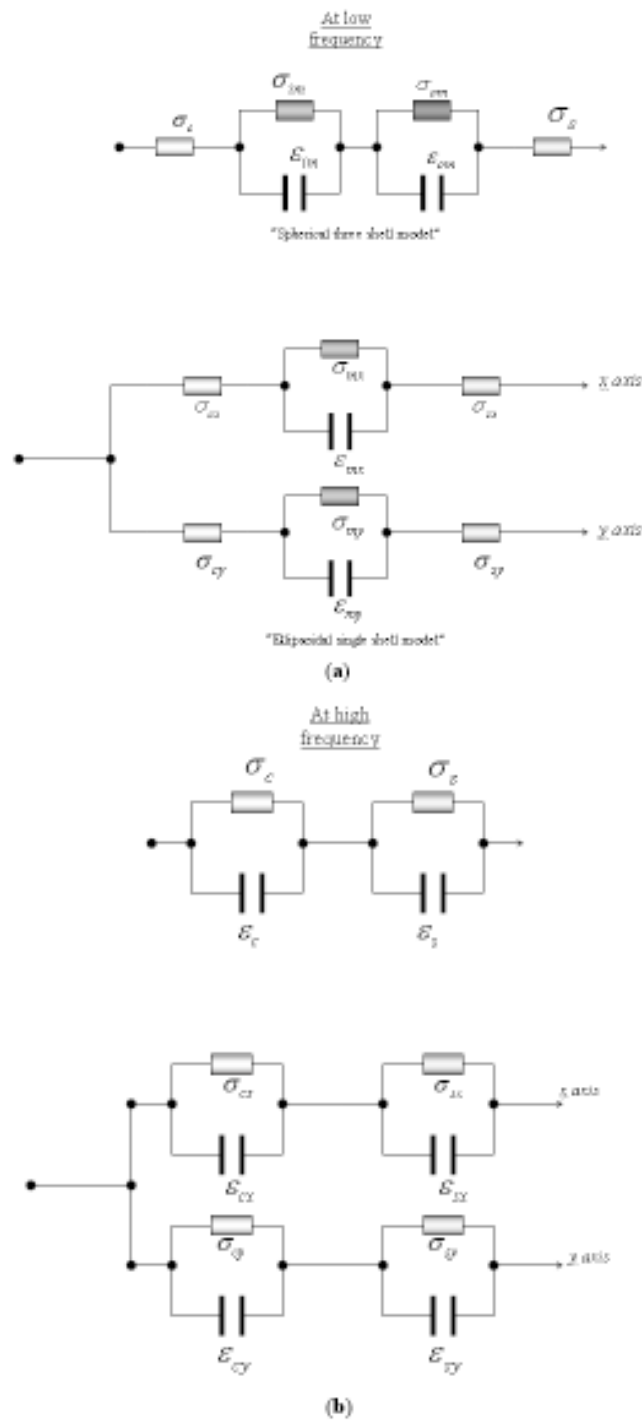


Figure 4. Simplification of the critical frequency of both models using presented presented schemes for the derivation of dielectrophoresis spectrum at low (a) and high (b) frequency ranges.

studies simple parallel cylinder electrodes (Zimmermann and Veinken, 1982; Mahaworasilpa et al., 1994) or round-tip electrodes may be used (Pohl and Crane, 1971; Zimmermann and Veinken, 1982). In ER studies four alternate-phase driven electrodes are commonly used (Gimsa et al., 1988; Gimsa et al., 1991; Fuhr et al., 1986).

In our earlier studies cylindrical nickel alloy electrodes with a diameter of 125 microns were used. They were aligned in parallel, 250 microns apart. The electrodes were dipped into the chamber containing the suspended cells after proper adjustment of the conductivity. Single cells were suspended in between the electrodes at the center of the chamber (Figure 5). An electric potential of 7 Vp-p was applied and the electric field intensity was 35-40 kilovolts/meter in the frequency range from kilohertz to megahertz. According to the electrode geometry the two components of the field intensity along the y and z axes can be expressed in vector and scalar forms $\vec{E}_{y,z} = \vec{E}_y + \vec{E}_z$ and $E_{y,z} = \sqrt{\vec{E}_y^2 + \vec{E}_z^2}$, respectively (Figure 6).

These electric field intensities were calculated in the same manner as Mahaworasilpa et al. (1994). Finally, the DEP translation of the cell was recorded with a digital video camera (Sony, CCD-IRIS, Japan) until it deposited at the electrodes.

c. Dielectrophoretic and angular velocities measurements

The cell's velocity during DEP was calculated from the observation of the video recordings on a TV monitor (Mitsubishi CT-29K1SB). By playing and replaying the video repeatedly, the position and displacement of the cell as it was moving towards an electrode were recorded. The data were plotted on a graph to determine the cell parameters by non-linear regression analysis. Once the distance along the z direction was obtained as a function of time (t), time differentiation was performed to determine the velocity function $v(t)$. This information was then

reentered into the function to obtain the experimental dielectrophoretic velocity (\vec{v}_{DEP}) for each position (Figure 7).

The theoretical velocity of an ellipsoidal single cell with mass (m) moving in suspending medium having viscosity of η can be written in the form

$$\vec{v}_{DEP} = \vec{\gamma} \left[\tanh \left(\frac{\beta t \sqrt{\vec{\gamma}}}{m} \right) \right]^2, \quad (11)$$

where $\vec{\gamma} = \frac{\vec{F}_{cell}}{\beta}$ and $\beta = 6\pi\eta aK$ where K is a shape factor defined as

$$K = \frac{\frac{4}{3}(\alpha^2 - 1)}{\frac{(2\alpha^2 - 1)}{(\alpha^2 - 1)^{1/2}} \ln[\alpha + (\alpha^2 - 1)^{1/2}] - \alpha}, \quad (12)$$

where $\alpha = \frac{b}{a}$. Under Newton's second law of motion, equation (9) can be simplified to $\vec{v}_{DEP} \approx \vec{\gamma}$. In another case of ER the angular velocity (ω) was determined in the same manner by counting the number of rotations over time and converting the number into radian /second.

Results

a. Theoretical profiles of Re[CMF]

The general appearances of the Re[CMF] and dielectrophoretic velocity curves plotted in the frequency range from 1 Hz to 1 GHz are quite similar. They are both bell shaped with 2 base areas, one in the negative frequency region and the other in the high frequency region. The peak of the curve has one turning point in the moderate frequency region which was shown to be the maximum positive value of the Re[CMF] (Figure 3). The results of the considering of the influence of all electrical parameters on these spectra are summarized below.

Changing the dielectric constant of the inner

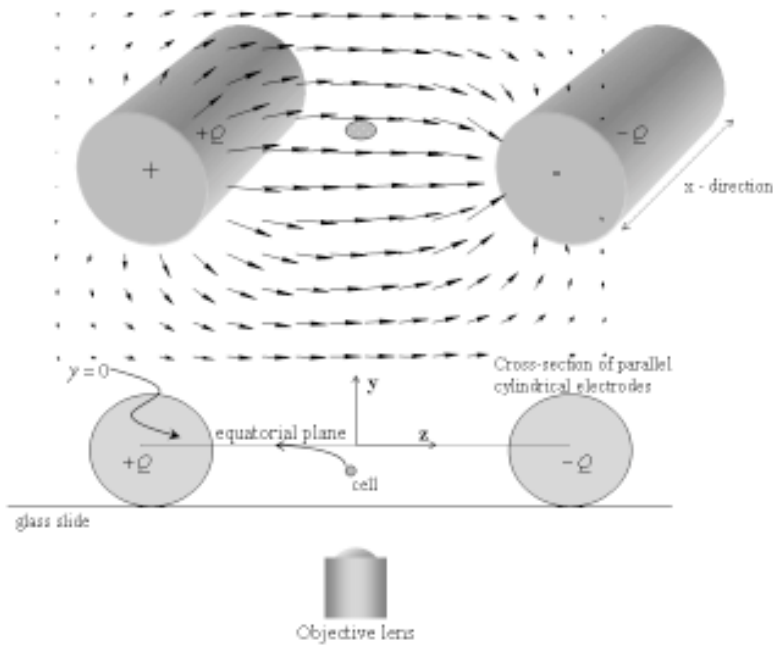


Figure 5. Cross-sectional view (not to scale) of the cell arrangement in the cell chamber used in the present study.

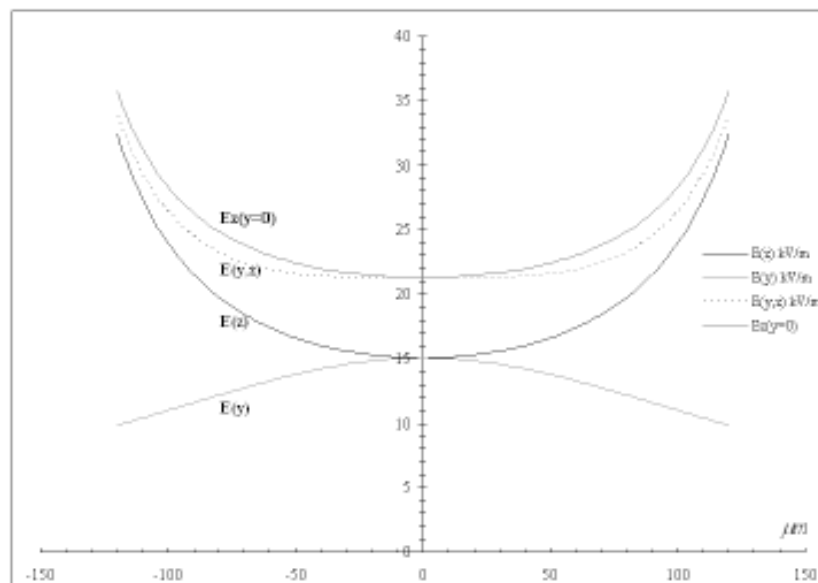


Figure 6. Electric field strengths along y and z axis between the two parallel electrodes were plotted as $E(y)$ and $E(z)$ including their summation of $E(y,z)$. Line of $E_z(y=0)$ represent electric field strength along z axis at equatorial plane with $y=0$.

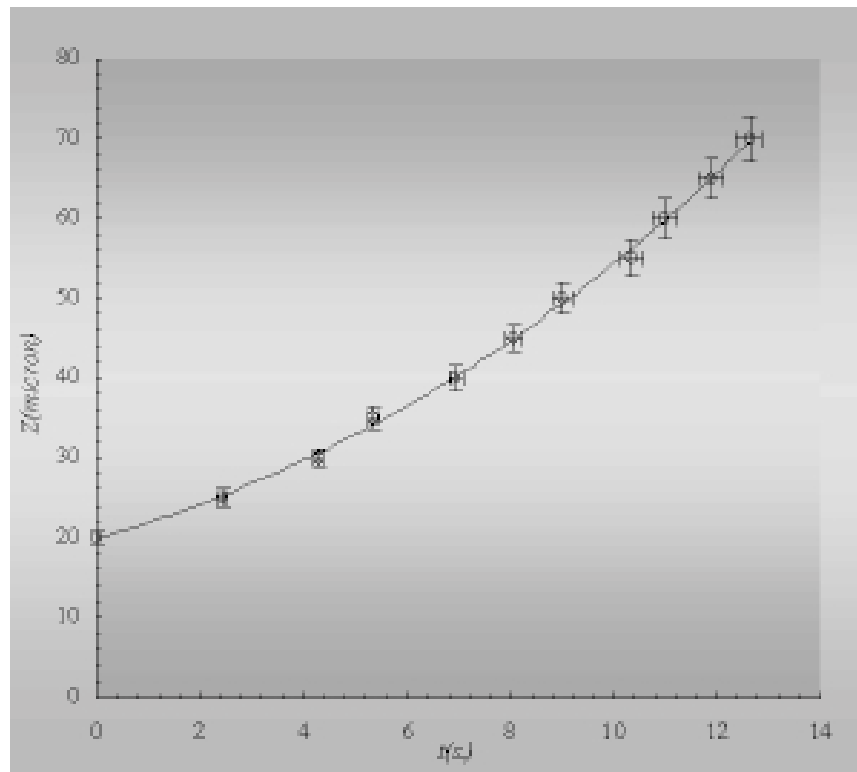


Figure 7. An example of plots of cell displacement as a function of time for the protoplast, sus-pended in 0.6 M mannitol, in between the parallel elec-trodes. A potential difference of 7 Vp-p was applied across the electrodes.

and outer membrane ($\epsilon_{im}, \epsilon_{om}$) in the range of 5 to 15 affects the spectrum in the lower frequency region (Figures 8a-1 and 8a-2). In contrast, it was found that changing the dielectric constant of the outer cytoplasm (ϵ_{oc}) to 50-70 ϵ_0 did not show a significant impact (Figure 8b-2). This means that ϵ_{oc} is not sensitive and does not affect the dipole moment of the model. Adjusting the conductivity of the inner cytoplasm (σ_{ic}) in the range from 0.1 to 1 $S.m^{-1}$ affects the spectrum in the high frequency range (the curve's shoulder) (Figure 8d-1). Thus, if the σ_{ic} increases, the spectrum moves towards higher frequencies. This, in turn, moves the spectrum towards lower frequencies. Similarly, changing the conductivity of the outer cytoplasm (σ_{om}) in the range of 0.1 to 1.0 $mS.m^{-1}$ affects the spectrum in

the lower frequency region (curve's base) (Figure 8c-2). If σ_{om} increases the base of the spectrum is shifted to the higher frequencies (Figure 8c-2). This results in a larger positive $Re[CMF]$ term and the f_{cl} moves to the higher frequency range as well. However, the effect of changing the dielectric properties of the outer cytoplasm (ϵ_{ic}) is limited to the base of the spectrum in the higher frequency range. Thus if increases, the base of the spectrum shifts the amplitude to larger positive values and slightly affects the f_{cl} (Figure 8b-1).

Cell radius changes affect the spectrum in the lower frequency region (curve's base and shoulder) (Figure 8e-1). Thus if the radius of the cell is larger, the shoulder of the curve shifts towards lower frequencies and the has a larger positive

value. This shifts the boundary of the lower frequency region towards lower frequencies as well. The effect of the cell radius on the spectrum at the curve's base is insignificant. This result is similar, though more pronounced, to that of changes in the thickness (Figures 8f-1 and 8f-2), dielectric constant ($\epsilon_m, \epsilon_{om}$) (Figures 8a-1 and 8a-2) and conductivity (σ_{om}) (Figure 8c-2) of the outer cell membrane.

A change in the thickness of the outer turning point of the curve's base at lower frequencies (Figure 8e-2). An increase in thickness slightly shifts the spectrum towards higher frequency. The thickness of the inner membrane δ_{im} affects the curve in the lower frequency region. Increasing δ_{im} shifts the shoulder of the curve towards lower frequencies (Figures 8f-1). This increases the magnitude of $\text{Re}[CMF]$ and decreases the boundary in the lower frequency range. These effects of all parameters on $\text{Re}[CMF]$ are relevant. The above considerations yield a better insight into the electric properties of cells.

b. Theoretical profiles of the critical frequencies

Theoretical plots in Fig.9a-d shows how changes in $\sigma_c, \sigma_m, \epsilon_c$ and ϵ_m affect the f_{cl} and f_{ch} values. These plots were obtained under fixed values of $\epsilon_m = 10\epsilon_0, \epsilon_c = 75\epsilon_0, \epsilon_s = 78\epsilon_0, \sigma_m = 10^{-7}, \sigma_c = 0.2 \text{ S.m}^{-1}$ and $a = 8, b = 6, c = 4 \text{ um}$. The L_k was assumed to be 0.272 when membrane thickness (δ) was 10 nm. The theoretical curves of f_{cl} and f_{ch} derived from an RC-model indicated that dielectric properties such as dielectric constant and conductivity of the cytoplasm and the membrane had obvious effects on the critical frequency. Critical frequency was also dependent on other factors such as depolarization factor (L_k) and the membrane thickness (δ) (Figures 10a and 10b).

c. Experimental results

It was found that yeast cell suspensions induced positive DEP at frequencies between 100 Hz to 1 MHz for σ_s between 3.5 mS.m^{-1} and 0.3 S.m^{-1} , respectively. The theoretical curves of f_{cl}

and f_{ch} derived from the RC-model agreed with experimental data (Figure 11). By fitting the theoretical curve with experimental data the dielectric constants (ϵ) and the conductivities (σ) of the membrane (m) and the cytoplasm (c) were revealed as $\epsilon_m = 10, \epsilon_c = 75, \sigma_m = 10^{-7}$ and $\sigma_c = 0.2 \text{ S.m}^{-1}$, respectively. The general appearance of the curves plotted in the whole frequency range from Hz to GHz is similar in shape to a "banana". Its length showed the maximum amplitude around 0.3 S.m^{-1} . Two curves were obtained with tips that merge when the value of the depolarization factor is properly adjusted (Gimsa and Wachner, 1999).

Discussion

The experimental results show that the peak of the real part of the dielectrophoretic spectrum has only one turning point in the medium frequency range (Figures 3 and 8). The experimental data of yeast cells represent a positive dielectrophoretic force, i.e. the cells were propelled towards the central electrode (Figure 5). In turn, the negative force repelled the cell from the central electrode. This negative dielectrophoresis mostly occurred in the kHz frequency range. The magnitude and direction of dielectrophoresis were fitted by the $\text{Re}[CMF]$. Actually, the cell was translocated with a constant velocity as Stokes' friction balances the force. Therefore, its velocity should be predicted from Newton's first law of motion; although the preferred motion was close to constant acceleration.

Fitting the theoretical curve to the experimental data points yielded the dielectric and conductance values as shown in Figure 11. Both the Laplace and the RC-model can be used for computing all functions involving the $\text{Re}[CMF]$ and $\text{Im}[CMF]$ of the spherical model. Each of the models consists of a number of parameters. The results yield the effects of these parameters on $\text{Re}[CMF]$ and $\text{Im}[CMF]$. As discussed above, the dielectric properties of the membrane are more prominent in the lower frequency range. On the other hand, those of the cytoplasm are visible in the high frequency range.

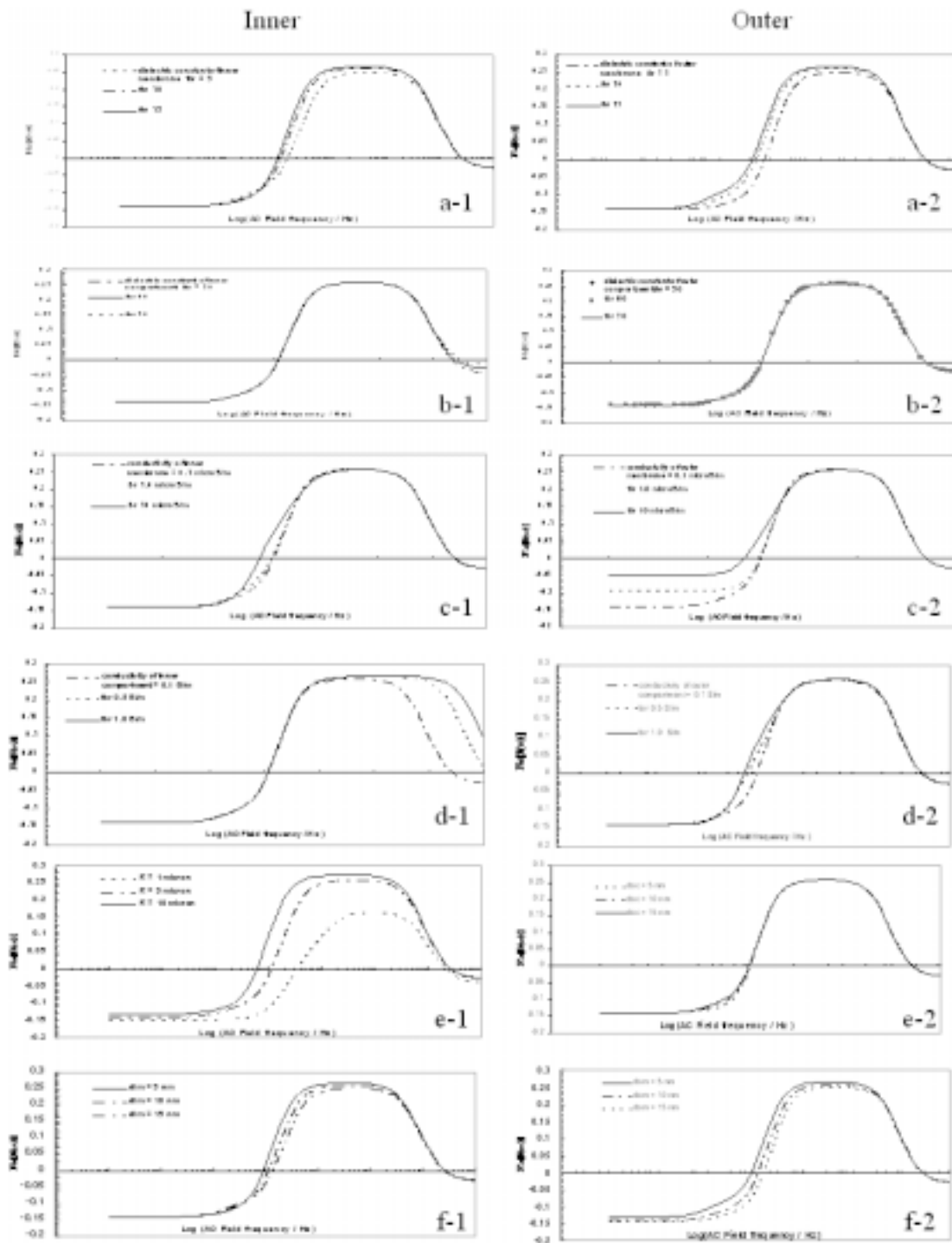


Figure 8. Theoretical plots show the dependence of $Re[f(w)]$ as a function of electric field frequencies. Effect of changes in the inner and outer compartments of ϵ_{im} , ϵ_{om} , ϵ_{ic} , ϵ_{oc} , σ_{im} , σ_{om} , σ_{ic} , σ_{oc} , R , δ_{oc} , δ_{im} and δ_{om} are shown in a-1, a-2, b-1, b-2, c-1, c-2, d-1, d-2, e-1, e-2, f-1 and f-2, respectively.

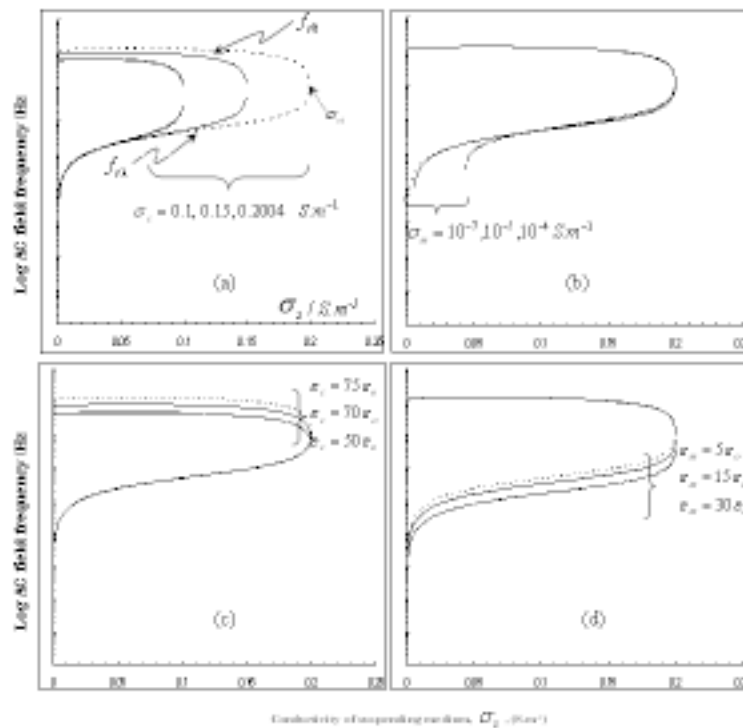


Figure 9. Theoretical plots show the dependence of the lower (f_{cl}) and the higher (f_{ch}) critical frequency as a function of medium conductivity (σ_s). Effect of changes in σ_c , σ_m , ϵ_c and ϵ_m are shown in (a) (b) (c) and (d), respectively.

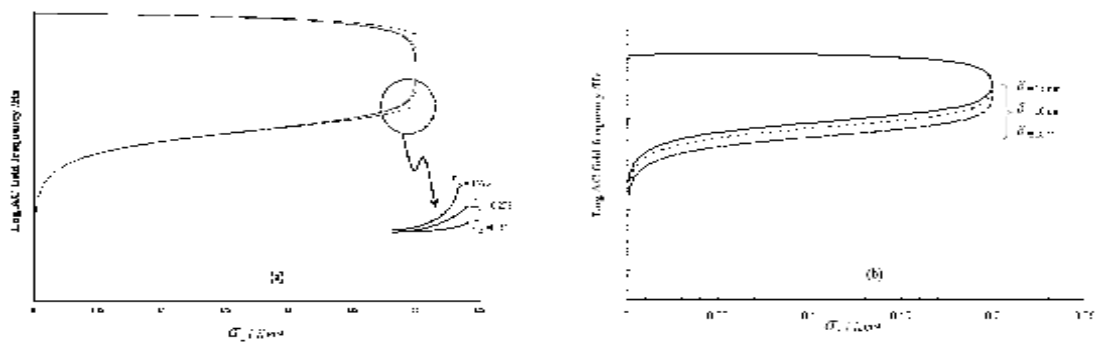


Figure 10. Theoretical plots show the dependence of the lower (f_{cl}) and the higher (f_{ch}) critical frequency as a function of medium conductivity (σ_s). Effect of changes in L_k and δ are shown in (a) and (b), respectively.

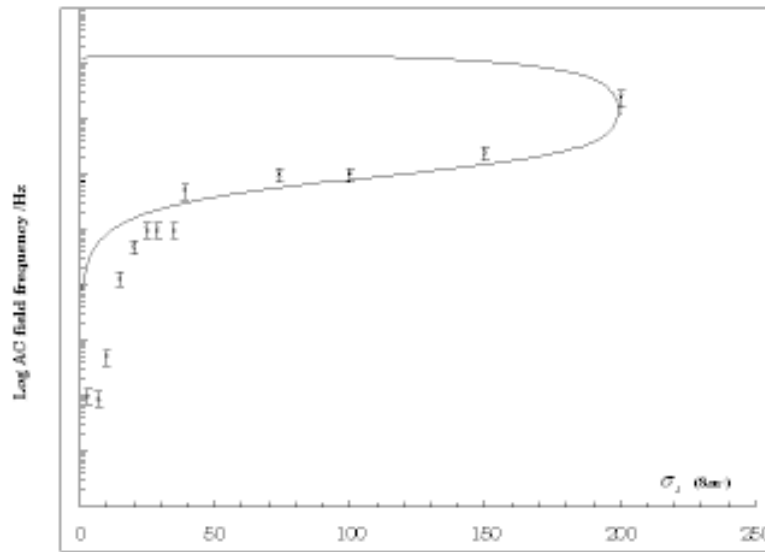


Figure 11. plots of f_{cl} against medium conductivity (σ_s) (circles with error bars) and theoretical plots for possible dielectric properties (solid line) of yeast cells. The estimated parameters are; $\epsilon_m = 10\epsilon_o$, $\epsilon_c = 75\epsilon_o$, $\epsilon_s = 78\epsilon_o$, $\sigma_m = 10^{-7}$ and $\sigma_c = 0.2 S.m^{-1}$.

Summary

We have reported two approaches for estimating the dielectric properties of cells. The conventional Laplace and the RC model were presented in this work. Nevertheless, the latter is more convenient to handle. The RC approach also provides an alternative to non-physicists in cell biotechnology. However, this very new approach has still not been verified with another ellipsoidal biological cell except for the human erythrocyte (Gimsa and Wachner, 1998), chicken red blood cells (Lippert and Gimsa, 2002) and yeast cells for this work. Moreover, some related experimental findings have not been included here, such as the reorientation of spheroid cells at certain frequencies (Lippert and Gimsa, 2002). This paper is, therefore, an overview of the concepts for those interested in this field and should help to avoid the repetition of investigations that have already been done. Nonetheless, further elaboration of these studies is possible. The two curves in Figure 10a for the lower and higher frequency ranges can be combined by

adjusting certain parameters to obtain new curves. Combining DEP, ER, EO, and ED techniques would be beneficial for further studies of dielectric cell properties.

Acknowledgements

The authors are grateful to Forschungsgemeinschaft Funk, Germany, for the financial support of SB during his work-stay at Rostock University (October 2004 - January 2005) and Prince of Songkla University for grant supporting this Ph.D project.

References

- Asami, K. and Irimajiri, A. 1984. Dielectric analysis of mitochondria isolated from rat liver II. Intact mitochondria as simulated by a double - shell model. *Biochim. Biophys. Acta*, 778: 570-578.
- Asami, K., Hanai, T. and Koizumi, N. 1980. Dielectric approach to suspensions of ellipsoidal particles covered with a shell in particular reference to

- biological cells. *Jpn. J. Appl. Phys.*, 19: 359-365.
- Asami, K., Yonezawa, T., Wakamatsu, H. and Koyanagi, N. 1996. Dielectric spectroscopy of biological cell. *Bioelectrochem Bioenerg*, 40: 141-145.
- Asami, K. 2002. Characterization of biological cells by dielectric spectroscopy. *Non-Crystal Solids*, 305: 268-277.
- Bunthawin, S., Butrat, P. and Boonlamp, M. 2003. Development of a computer program to investigate electrical properties of Phuket pineapple leaf single cells by using dielectrophoresis. *Songklanakarin J. Sci. Technol.*, 25: 227-237.
- Bunthawin, S. and Boonlamp, M. 2005. Development of a single cells spherical shell model for an investigation of electrical properties with computing program. *Songklanakarin J. Sci. Technol.*, 27: 393-416.
- Lippert, S. and Gimsa, J. 2002. High resolution measurements of dielectric cell properties by a combination of AC-electrokinetic effects. In: 2nd International Workshop on Biological effects of EMFs at Rhodes Greece. 7-11 October 2000, 830-836.
- Gheorghiu, G. 1996. Measuring living cells using dielectric spectroscopy. *Bioelectro. Bioenerg*, 40: 387-401.
- Gimsa, J., Glaser, R. and Fuhr, G. 1988. Remarks on the field distribution in four electrode chambers for electrorotational measurements. *Studia Biophysica.*, 125: 71-76.
- Gimsa, J., Marszalek, P., Loewe, U. and Tsong, T. 1991. Dielectrophoresis and electrorotation of neurospora slime and murine myeloma cells. *Biophys. J.*, 60:749-760.
- Gimsa, J., Muller, T., Schnelle, T. and Fuhr, G. 1996. Dielectric spectroscopy of single human Erythrocytes at physiological ionic strength: Dispersion of the cytoplasm. *Biophys J.*, 71: 495-506.
- Gimsa, J. and Wachner, D. 1998. A unified resistor-capacitor model for impedance, dielectrophoresis, electrorotation and induced transmembrane potential. *Biophysical J.*, 75: 1107-1116.
- Gimsa, J. and Wachner, D. 1999. A polarization model overcoming the geometric restrictions of the Laplace solution for spheroidal cells: Obtaining new equations for field-induced forces and transmembrane potential. *Biophysical J.*, 77: 1316-1326.
- Gimsa, J. 2001. A comprehensive approach to electro-orientation, electrodeformation, dielectrophoresis, and electrorotation of ellipsoidal particles and biological cells. *Bioelectrochem J.*, 54: 23-31.
- Fuhr, G. and Kuzmin, P.I. 1986. Behaviour of cells in rotating electric fields with account to surface charges and cell structures. *J. Biophysics*, 50: 789-795.
- Fuhr, G., Glaser, R. and Hagedorn, R. 1986. Rotation of dielectrics in a rotation electric high-frequency field. *J. Biophysics*, 49: 395-402.
- Jones, T. B. 1995. *Electromechanics of Particles*. Cambridge University Press, Cambridge, pp 2.
- Jones, T. B. 2003. Basic theory of dielectrophoresis and electrorotation, *IEE E Engineering in medicine and biology magazine*, Nov/Dec 2003: 33-42.
- Kaler, K.V.I.S. and Jones, T.B. 1990. Dielectrophoretic spectra of single cells determined by feedback-controlled levitation. *Biophys. J.* 57: 173-182.
- Kakutani, T., Shibatani, S. and Sugai, M. 1993. Electrorotation of non-spherical cells: theory for ellipsoidal cells with an arbitrary number of the shells, *J. Bioelectrochem. Bioenerg.*, 31: 131-145.
- Mahaworasilpa, T., Coster, H.G.L. and George, E.P. 1994. Force on biological cells due to Applied (AC) electric fields. I. Dielectrophoresis. *Biochim. Biophys. Acta.*, 1193: 118-126.
- Mahaworasilpa, T., Coster, H.G.L. and George, E.P. 1996. Force on biological cells due to applied (AC) electric fields. II. Electro-rotation. *Biochim. Biophys. Acta.*, 1281: 5-14.
- Marszalek, P., Zienlinsky, J.J., Fikus, M. and Tsong, T.Y. 1991. Determination of electric parameters of cell membranes by a dielectrophoresis method. *Biophys. J.*, 59: 982-987.
- Pohl, H. A. 1978. *Dielectrophoresis : The Behaviour of Neutral Matter in Non-Uniform Electric Fields*. Cambridge University Press, Cambridge. pp 6.
- Pohl, H. A. and Crane, J.S. 1971. Dielectrophoresis of

- cells. *Biophys. J.*, 11: 711-727.
- Radu, M., Petcu, I., Sommer, A. and Avram, D. 1996. Change in membrane electrical parameters of yeast following chemical treatment for protoplast isolation. *J. Bioelec-trochem Bioenerg.*, 40: 159-166.
- Scher, L.D. 1968. Dielectrophoresis in lossy dielectric media. *Nature*, 220: 695-696.
- Schwan, H.P. 1988. Dielectric spectroscopy and electrorotation of biological cells. *Ferroelectrics J.*, 86: 205-223.
- Saito, M., Schwan, H.P. and Schwarz, G. 1966. Response of nonspherical biological particles to alternating electric fields. *Biophys. J.*, 6: 313-327.
- Sudsiri, J. Wanichapichart, P., Mahaworasilpa, T. and Coster, H.G.L. 1999. AC electric field frequencies for isolating five marine phytoplanktons. *Songklanakarin J. Sci. Technol.*, 21(2): 213-219.
- Watanabe, M., Toshinobu, S. and Irimajiri, A. 1991. Dielectric behavior of the frog lens in the 100Hz to 500 MHz range: Simulation with an allocated ellipsoidal-shells model. *Biophys. J.*, 59: 139-149.
- Zimmermann, U. and Vienken, J. 1982. Electric field induced cell to cell fusion. *J. Membrane Biol.*, 67: 165-182.